frontiers in
PSYCHIATRY

ORIGINAL RESEARCH ARTICLE
published: 11 January 2012
doi: 10.3389/fpsyt.2011.00083

Resting state functional connectivity correlates of inhibitory control in children with attention-deficit/hyperactivity disorder

Maarten Mennes[1†], Natan Vega Potler[1†], Clare Kelly[1], Adriana Di Martino[1], F. Xavier Castellanos[1,2] and Michael P. Milham[2,3]*

[1] *Phyllis Green and Randolph Cowen Institute for Pediatric Neuroscience, NYU Langone School of Medicine, NYU Child Study Center, New York, NY, USA*
[2] *Nathan Kline Institute for Psychiatric Research, Orangeburg, NY, USA*
[3] *Center for the Developing Brain, Child Mind Institute, New York, NY, USA*

Edited by:
Alex Fornito, University of Melbourne, Australia

Reviewed by:
Damien Fair, Oregon Health and Science University, USA
Jessica A. Church, Washington University School of Medicine, USA

****Correspondence:***
Michael P. Milham, Child Mind Institute, 445 Park Avenue, New York, NY 10022, USA.
e-mail: michael.milham@childmind.org

[†]Maarten Mennes and Natan Vega Potler have contributed equally to this work.

Motor inhibition is among the most commonly studied executive functions in attention-deficit/hyperactivity disorder (ADHD). Imaging studies using probes of motor inhibition such as the stop signal task (SST) consistently demonstrate ADHD-related dysfunction within a right-hemisphere fronto-striatal network that includes inferior frontal gyrus and pre-supplementary motor area. Beyond findings of focal hypo- or hyper-function, emerging models of ADHD psychopathology highlight disease-related changes in functional interactions between network components. Resting state fMRI (R-fMRI) approaches have emerged as powerful tools for mapping such interactions (i.e., resting state functional connectivity, RSFC), and for relating behavioral and diagnostic variables to network properties. We used R-fMRI data collected from 17 typically developing controls (TDC) and 17 age-matched children with ADHD (aged 8–13 years) to identify neural correlates of SST performance measured outside the scanner. We examined two related inhibition indices: stop signal reaction time (SSRT), indexing inhibitory speed, and stop signal delay (SSD), indexing inhibitory success. Using 11 fronto-striatal seed regions-of-interest, we queried the brain for relationships between RSFC and each performance index, as well as for interactions with diagnostic status. Both SSRT and SSD exhibited connectivity–behavior relationships independent of diagnosis. At the same time, we found differential connectivity–behavior relationships in children with ADHD relative to TDC. Our results demonstrate the utility of RSFC approaches for assessing brain/behavior relationships, and for identifying pathology-related differences in the contributions of neural circuits to cognition and behavior.

Keywords: ADHD, connectivity, intrinsic architecture, transition zones, rest, fMRI, interaction

INTRODUCTION

Emerging models of attention-deficit/hyperactivity disorder (ADHD) pathophysiology highlight disease-related alterations in functional interactions among multiple brain regions, extending the traditional focus on frontal–striatal dysfunction (Dickstein et al., 2006). Using resting state functional connectivity (RSFC) as an index of functional interactions, studies have demonstrated ADHD-related abnormalities in the interactions among brain regions supporting the implementation and maintenance of attentional control [e.g., dorsal anterior cingulate cortex (dACC) and insula; Tian et al., 2006]. ADHD-related constraints in the segregation of processing between attentional control regions and those implicated in *internal mentation* (i.e., the default network) have been demonstrated (Castellanos et al., 2008), as well as ADHD-related differences in functional connectivity within the default network itself (Fair et al., 2010; Chabernaud et al., in press). Reminiscent of developmental immaturity (Fair et al., 2008), these findings have intrigued researchers and invigorated new avenues of inquiry. Yet, little has been done experimentally to bridge emerging dysconnectivity models with existent neuropsychological models of ADHD.

Here, we take a first step toward linking neuropsychological and dysconnectivity models of ADHD. In particular, we focus on impaired inhibitory control, commonly considered a hallmark of ADHD (Nigg, 2001). Previously, task-based imaging studies using common behavioral probes of inhibitory control such as the Go–No Go and stop signal task (SST) have implicated fronto-striatal circuitry in ADHD (Nigg, 1999; Konrad et al., 2000; Aron and Poldrack, 2005). Specifically, they revealed hypoactivation in a predominantly right-hemispheric network encompassing the inferior frontal gyrus/anterior insula, pre-supplementary motor area (pre-SMA), dACC, thalamus, and caudate nucleus (Rubia et al., 1999; Aron and Poldrack, 2005; for a review see Dickstein et al., 2006; Cubillo et al., 2010). In the present work, we related inter-individual differences in SST performance to differences in connectivity observed for fronto-striatal regions-of-interest (ROI). In addition, we assessed the modulatory effect of the presence or absence of an ADHD diagnosis on such relationships.

We focused on inhibitory measures obtained during SST performance. The SST is a common probe for inhibitory control, requiring inhibition of a prepotent Go response upon presentation of an auditory stop signal. Two performance measures related to inhibitory control can be derived from the SST. (1) The stop signal delay (SSD) is the average delay between stimulus presentation and presentation of the auditory stop signal. Across "stop trials," the SSD is titrated based on the participant's inhibitory success. (2) The stop signal reaction time (SSRT) is an index of inhibitory process speed, and is estimated by subtracting the mean SSD from the mean go reaction time. While increased SSRT in ADHD is commonly interpreted as less efficient inhibitory control, higher SSRT in ADHD may also reflect slower and more inconsistent motor responses and visual stimulus processing (Alderson et al., 2007, 2008). Finding that children with ADHD exhibited slower SSRT and Go reaction times, but not shorter SSD, Alderson and colleagues concluded that children with ADHD exhibited motor slowing or general inattention rather than a primary inhibition deficit (see also Castellanos et al., 2006). This prompted the recommendation that SSD be included as an additional measure of motor inhibition given its more direct link to inhibitory success (Alderson et al., 2007, 2008). Indeed, in tracking versions of the SST (such as the one we used), the SSD is adjusted on every stop trial depending on whether the participant successfully inhibited his/her response on the previous stop trial.

Both SST inhibition performance measures (SSD, SSRT), obtained outside the MRI scanner, were related to RSFC measured during functional MRI scans in which participants were simply directed to rest. In particular, we investigated patterns of functional connectivity related to 11 fronto-striatal brain ROI implicated in inhibitory control (Boehler et al., 2010).

MATERIALS AND METHODS

PARTICIPANTS

Sixty-three children, including typically developing children (TDC) and children with ADHD, completed the SST task and a resting state scan session. Eighteen participants were excluded from further analyses due to SST Go trial accuracy < 75% (Nigg, 1999), and five more because of excessive motion during the resting state scan (see fMRI Image Preprocessing). In addition, six participants were excluded because their performance was >2 SD beyond the mean on a behavioral performance variable (SSRT, SSD, mean reaction time, or reaction time coefficient of variation). Our intent was to include only those children who could be confidently regarded as having followed task instructions.

Consequently, data from 34 children (aged 8–13 years) were analyzed in the current study (**Table 1** shows participant characteristics). Seventeen children were TDC (mean age 10.8 years) and 17 were diagnosed with ADHD (mean age 11 years). Within TDC 47% were female, in contrast with 18% females in the ADHD group ($\chi^2_{(1)} = 5.4$, $p = 0.015$). Children with ADHD and TDC exhibited similar estimates of full IQ indexed by the Wechsler Abbreviated Scale of Intelligence (WASI).

Typically developing children had no past or present DSM-IV-TR axis-I diagnosis or neurological illness nor history of treatment with psychotropic medications, as confirmed by parent administration of the Schedule of Affective Disorders and Schizophrenia for Children – Present and Lifetime Version (Kaufman et al., 1997; KSADS-PL). Children with Combined type ADHD ($n = 11$) and predominantly Inattentive type ADHD ($n = 6$) were included. Clinicians' DSM-IV-TR ADHD diagnoses were based on KSADS-PL interview. Four children with ADHD had comorbid oppositional defiant disorder, and one had comorbid adjustment disorder with depressive mood. Children with ADHD were excluded if they had a diagnosis of pervasive developmental disorders, psychosis or major depression or if they were treated with any non-stimulant psychotropic medications within the month prior to participation (3 months for neuroleptics). Only children with an estimated full IQ above 80 were included. Twelve children with ADHD (66%) were medication-naïve. Three children with ADHD currently treated with stimulant were asked to discontinue their medication 72 h prior to the scan session. Two remaining children were not treated with stimulants at the time of the study, but were treated at earlier points in their life. Finally, we obtained Conners Parent Rating Scale-Revised:Long Version (CPRS-R:L; Conners et al., 1998) scores for all participants. The CPRS-R:L is a widely used, normed parent questionnaire that assesses problems related to conduct, hyperactivity–impulsivity, and inattention as well as a range of other psychopathology.

As part of a 1-h scan session, all participants completed at least one 6.5 min resting state scan as well as a high-resolution anatomical scan (MPRAGE). After the scan session each participant completed a SST (Nigg, 1999) outside the scanner.

Table 1 | Participant characteristics and behavioral performance scores obtained from the stop signal task (SST).

	ADHD	TDC	*p*-Value
N	17; 3 female/14 male	17; 8 female/9 male	<**0.02**
Age	11.0 ± 1.26	10.8 ± 1.92	0.87
IQ	111.8 ± 14.26	112.1 ± 14.11	0.95
Mean go RT	629.9 ± 54.25	637.5 ± 62.97	0.35
Go RT CV	0.24 ± 0.02	0.23 ± 0.03	0.37
SSRT	299.1 ± 46.25	263.2 ± 63.94	<**0.03**
SSD	330.8 ± 73.26	374.3 ± 108.56	0.09
Go accuracy	0.89 ± 0.04	0.91 ± 0.05	0.23
Stop accuracy	0.52 ± 0.03	0.54 ± 0.05	0.21
CPRS-R			
DSM-IV total	71.24 ± 9.16	44.24 ± 4.58	<**0.01**
DSM-IV inattentive	71.00 ± 9.37	43.47 ± 3.76	<**0.01**
DSM-IV hyperactive/impulsive	67.53 ± 12.43	46.18 ± 5.33	<**0.01**
Cognitive problems/inattention	69.59 ± 8.69	43.76 ± 3.25	<**0.01**
Hyperactivity	65.29 ± 14.25	45.00 ± 2.78	<**0.01**
ADHD Index	72.59 ± 8.02	44.24 ± 3.73	<**0.01**

Go, Go trials; RT, reaction time; CV, coefficient of variation; SSRT, stop signal reaction time; SSD, stop signal delay; Stop, stop trials. p-Values for the SST behavioral measures and the Conners Parent Rating Scale-Revised (CPRS-R) measures are based on one-tailed t-tests. A significance level of $p < 0.05$ was used for all comparisons.

fMRI DATA ACQUISITION

Data were collected on a Siemens Allegra 3.0 Tesla scanner. All participants completed at least one 6.5 min long resting state fMRI (R-fMRI) scan (180 EPI volumes, TR = 2000 ms, TE = 25 ms, flip angle = 90°, 33 slices, voxels = 3 mm × 3 mm × 4 mm). All participants were instructed to rest with their eyes open during the scan. For spatial normalization and localization purposes we also acquired a high-resolution T1-weighted anatomical image (MPRAGE, TR = 2530 ms; TE = 3.25 ms; TI = 1100 ms; flip angle = 7°; 128 slices; FOV = 256 mm; voxel-size = 1 mm × 1.3 mm × 1.3 mm). Finally, a field map and short-TE EPI scan were also acquired to improve functional-to-anatomical co-registration.

STOP SIGNAL TASK

The SST is a computerized visual choice reaction time task aimed at examining inhibitory control (Logan et al., 1997; Nigg, 1999). On each trial an "X" or "O" was visually presented. Participants were required to respond as quickly and accurately as possible to the "X" or "O" by pressing "Enter" or "O," respectively. Each visual stimulus was displayed on the screen for 1000 ms. Trials were separated by a 500-ms display of a fixation cross and a 1000-ms blank screen. The SST comprised 80% Go trials and 20% Stop trials. On Go trials, participants were required to respond to the visual stimulus. In contrast, on Stop trials, an auditory stop stimulus was presented after the visual stimulus, indicating that participants had to inhibit their response. The delay between the visual stimulus and auditory stop stimulus (SSD) started at 250 ms. If participants successfully inhibited the prepotent Go response, the SSD on the next stop trial was increased by 50 ms, making inhibition more difficult on the next stop trial. If the participant failed to inhibit, the SSD on the next stop trial was decreased by 50 ms, i.e., the auditory tone was presented sooner, making inhibition easier. This procedure was implemented to attain a SSD at which participants were able to successfully inhibit 50% of the Stop trials. Based on the horse-race model (Logan et al., 1984), which posits a race between the go and inhibition processes, the process that finishes first gets executed. In successful stop trials the inhibition process is able to catch up and override the go process, while in unsuccessful stop trials the go response is executed before the inhibition process finishes. Based on this theory, titrating the SSD to obtain a 50% inhibition success rate makes it possible to obtain an estimate of the length of the inhibition process (SSRT) by subtracting the mean SSD from the mean Go reaction time. A smaller SSRT indicates a faster inhibition process. A smaller SSD indicates less successful inhibition, as participants require a shorter delay between the go stimulus and the stop signal to achieve successful inhibition. The SSRT and SSD thus form two related inhibitory indices of interest. After two practice blocks, all participants completed six task blocks. Each block comprised 32 trials: 24 go trials and 8 stop trials.

fMRI IMAGE PREPROCESSING

Data processing was performed using Analysis of Functional NeuroImaging[1] (AFNI) and FMRIB Software Library[2] (FSL). Image preprocessing consisted of discarding the first 4 EPI volumes from each resting state scan to allow for signal equilibration; slice time correction for interleaved acquisitions; 3-D motion correction with Fourier interpolation; despiking (detection and removal of extreme time series outliers); spatial smoothing using a 6-mm FWHM Gaussian kernel; mean-based intensity normalization of all volumes by the same factor; temporal bandpass filtering (0.009–0.1 Hz); and linear and quadratic detrending. FSL FLIRT was used for linear registration of the high-resolution structural images to the MNI152 template (Jenkinson and Smith, 2001; Jenkinson et al., 2002). This transformation was then refined using FNIRT non-linear registration (Andersson et al., 2007). Linear registration of each participant's functional time series to the high-resolution structural image was performed using FLIRT. This functional-to-anatomical co-registration was improved by intermediate registration to a low-resolution image and b0 unwarping.

We did not analyze participants who exhibited >4 mm maximum displacement between consecutive timepoints in their resting state scans as movement artifacts may affect resting state analyses (Van Dijk et al., 2012; Power et al., in press). When possible we analyzed the first resting state scan of the scan session. The first resting state scan was analyzed for all but one participant, whose first scan contained excessive motion. The second resting state scan was used for that participant. As indicated by the data shown in **Table 2**, our final sample contained limited motion artifacts, and children with ADHD did not differ from TDC in motion parameters. To remove between-participant variance related to differences in motion, we included the root mean square (RMS) of the maximum displacement between consecutive timepoints in the resting state scan as a covariate in all group-level analyses. Finally, in an effort to minimize the impact of motion artifacts, Power et al. (in press) propose removing timepoints containing movement artifacts from each

Table 2 | Mean ± SD for movement parameters calculated for the resting state scans.

	TDC	ADHD	*p*-Value
RMS mean relative displacement[v]	0.03 (±0.03)	0.03 (±0.02)	0.39
RMS maximum relative displacement[v]	0.23 (±0.30)	0.35 (±0.45)	0.18
N relative displacements >0.1 mm[v#]	8.65 (±12.7)	7.88 (±9.34)	0.42
Framewise displacement[p]	0.13 (±0.10)	0.12 (±0.07)	0.42
N framewise displacements >0.5 mm[p#]	4.53 (±8.99)	5.06 (±6.61)	0.85

Movement was calculated as the displacement between two consecutive timepoints (i.e., relative or framewise displacement). p-Values are indicated for one-sided unpaired t-tests between TDC and ADHD. RMS: Root Mean Square. [v]Measures derived from Van Dijk et al. (2012). [p]Measures derived from Power et al. (in press). [#]There were 180 available timepoints for every participant. As such, 10 displacements correspond to 5.5% of all timepoints and 5 displacements correspond to 3% of all timepoints.

[1] http://afni.nimh.nih.gov/afni
[2] www.fmrib.ox.ac.uk

participant's time series. Accordingly, we also repeated our analyses removing timepoints that exhibited micromovements exceeding 0.5 mm. As described in the supplementary material accompanying this paper, removing these timepoints did not alter our results.

NUISANCE SIGNAL REGRESSION

To control for the effects of motion and physiological processes (i.e., cardiac and respiratory fluctuations) at each timepoint, each participant's 4-D preprocessed volume was regressed with nine predictors that modeled white matter, cerebrospinal fluid, the global signal, and six motion parameters. The resultant 4-D residuals volumes were used in all subsequent analyses.

SEED SELECTION

We selected 11 seed ROIs from a recent study that attempted to improve the two most commonly used contrasts in SST-based fMRI investigations, namely comparing successful to unsuccessful stop trials and comparing successful stop to successful go trials (Boehler et al., 2010). As those authors note, the former approach is overly conservative, as it is not sensitive enough to measure the influence of inhibitory control in unsuccessful stop trials, while the latter approach does not account for the differential sensory requirements of the two trial types. Instead, Boehler and colleagues examined regions implicated in inhibitory control during successful as well as unsuccessful inhibitory trials, taking into account potential differences in sensory requirements. To this end they modeled a second-level conjunction contrast that included a comparison of successful and unsuccessful stop trials versus go trials, as well as a comparison of successful and unsuccessful stop trials versus stimulus-irrelevant stop trials. The stimulus-irrelevant stop trials shared the same sensory stimuli as the normal stop trials, but consisted of a passive viewing block.

We created spherical seeds (radius = 4 mm) centered on 11 different regions of the functional network implicated in response inhibition, as defined by the second-level conjunction analysis from Boehler et al. (see Table 5 in Boehler et al., 2010). Three coordinates of peak activity in the left insula that were less than 8 mm apart were averaged to avoid inclusion of redundant seed regions in our analysis. In addition, the left thalamus coordinates were adjusted to avoid partial voluming effects because the seed placed at the original coordinates included CSF voxels. Seed names and their coordinates are shown in **Table 3**. **Figure 1** displays the seeds on brain surface renderings.

PARTICIPANT-LEVEL ANALYSES

After extracting the mean time series for each seed in MNI152 2 mm standard space, we calculated whole-brain functional connectivity maps in native space by correlating the mean seed time series with the time series of every other voxel in the brain using AFNI 3dfim+. This produced participant-level correlation maps of voxels in the brain that positively or negatively correlated with the mean times series of each seed. The correlation maps were Fisher-z transformed to improve normal distribution and transformed into MNI152 2 mm × 2 mm × 2 mm standard space for further group-level analyses.

Table 3 | MNI152 standard space coordinates for seed regions used in the functional connectivity analyses.

Seed ROI	Hemisphere	MNI coordinates (*x, y, z*)		
Frontal operculum	R	50	18	0
Insula	R	42	10	−6
Insula[a]	L	−34	18	2
Pre-SMA	R	2	14	50
ACC	L/R	0	26	22
Supramarginal gyrus	R	58	−44	30
Mid-occipital gyrus	L	−32	−88	−2
Caudate	L	−8	16	6
Caudate	R	8	12	2
Thalamus	R	2	−20	2
Thalamus[b]	L	−4 (−2)	−16 (−12)	0 (0)

Seeds were selected from Boehler et al. (2010). [a]To avoid inclusion of redundant seed ROIs we averaged the coordinates of three insula seeds located near each other. [b]To avoid effects of partial voluming due to the fact that a seed placed at the original coordinates included CSF voxels, we adjusted the coordinates of the left thalamus seed. Original coordinates are shown between parentheses.

GROUP-LEVEL ANALYSES

Group-level mixed-effects analyses for each seed ROI were performed using FSL FEAT[3]. We assessed the relationship between RSFC and inhibition performance on the SST, as well as a possible interaction of this relationship with diagnosis. To this end we modeled diagnosis, SSRT, SSD, and a diagnosis-by-behavior interaction (obtained by multiplying diagnosis with the behavioral variables) for each SSRT and SSD in a two-sample t-test. Age, sex, maximum RMS displacement, and FIQ were included as covariates. While SSRT and SSD were highly correlated ($r = -0.81$), tolerance $[(1-r^2) = 0.32]$, and a variance inflation factor of 3.1 support the validity of including both measures in the same model.

We also investigated the effect of diagnosis in a two-sample t-test. Age, sex, maximum RMS displacement, and FIQ were again included as covariates. For all analyses, correction for multiple comparisons was carried out at the cluster level using Gaussian random field theory (voxel-wise: minimum Z-score > 2.3; $p < 0.05$ corrected).

RESULTS

BEHAVIORAL RESULTS

Replicating previous findings, children with ADHD exhibited significantly higher SSRT relative to TDC (one-tailed unpaired t-test $p = 0.03$; **Figure 2**; **Table 1**). Although not significant, we observed marginally lower SSD in ADHD relative to TDC ($p = 0.09$, one-tailed; **Figure 2**). No significant differences were observed for mean Go reaction time ($p = 0.35$), Go reaction time coefficient of variation ($p = 0.37$), Go trial accuracy ($p = 0.23$), or stop trial accuracy ($p = 0.21$; see **Table 1**).

CONNECTIVITY–BEHAVIOR RELATIONSHIPS ACROSS PARTICIPANTS

Regression analysis revealed a significant relationship between differences in SSRT among participants and inter-individual

[3]http://fsl.fmrib.ox.ac.uk/fsl/feat5

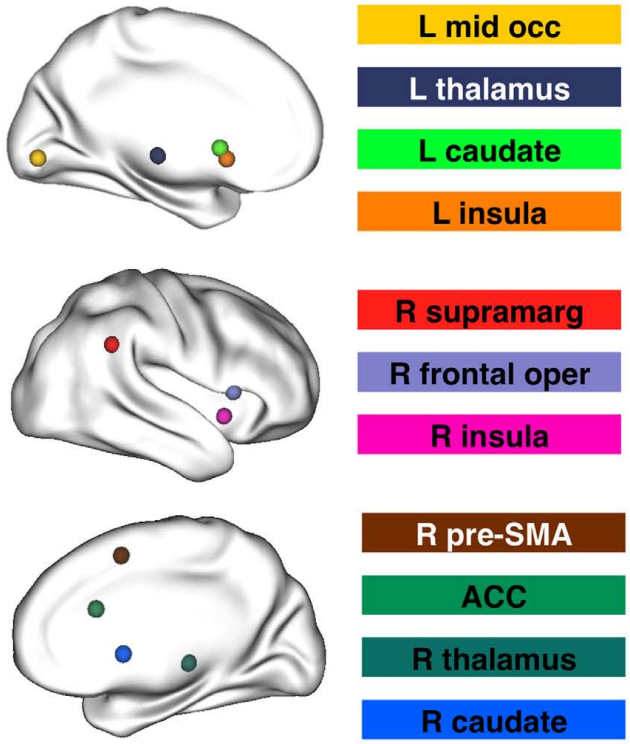

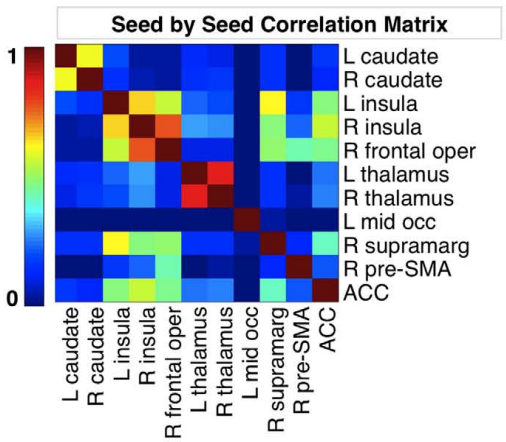

FIGURE 1 | Seed ROI used for functional connectivity analyses. The 11 seed regions were derived from Boehler et al. (2010) and are based on a conjunction analysis that assessed inhibitory control in the stop signal task (SST). The matrix at the bottom of the figure illustrates the seed by seed correlations for the typically developing children in our study. There was no effect of diagnosis on the seed by seed correlations, nor were the correlations related to the SST performance measures. R, right; L, left; mid occ, middle occipital gyrus; supramarg, supramarginal gyrus; pre-SMA, pre-supplementary motor area; ACC, anterior cingulate cortex.

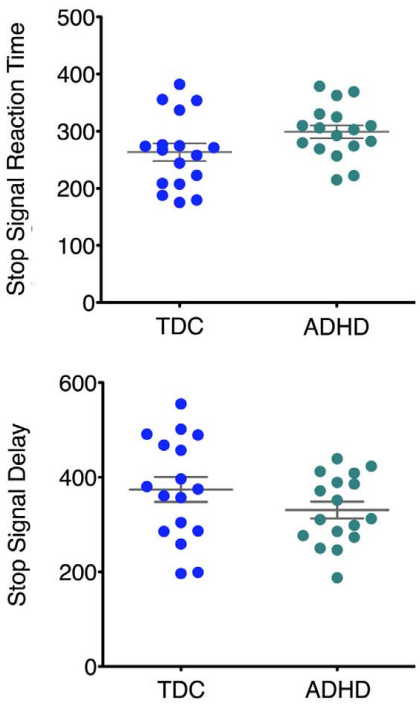

FIGURE 2 | Main effect of ADHD on SSRT ($p < 0.03$) and SSD ($p = 0.09$). Gray lines indicate mean ± SE.

variation in the functional connectivity networks of the anterior cingulate cortex, right pre-SMA, and right thalamus seeds (see **Figure 3**; **Table 4** lists the peak coordinates for each significant cluster). Specifically, higher SSRT (slower inhibition process) was associated with increased positive connectivity between right thalamus and anterior cingulate cortex. A similar effect was observed for the ACC and pre-SMA seeds ($Z > 2.3$; $p < 0.05$, corrected). The significant cluster observed for the pre-SMA seed further extended into left superior frontal gyrus. Finally, we also observed a significant positive SSRT-connectivity relationship between the right thalamus seed and left putamen.

Differences in SSD among participants were related to inter-individual variation in the functional connectivity networks of right caudate and pre-SMA (**Figure 3**). Longer SSD were associated with increased *positive* connectivity between pre-SMA and anterior cingulate cortex/left superior frontal gyrus. In contrast, increased *positive* connectivity between pre-SMA and right middle frontal gyrus was associated with shorter SSD. Shorter SSD were also associated with increased *negative* functional connectivity between the right caudate seed and left intracalcarine cortex.

As shown in **Figure 4**, the clusters exhibiting a significant positive connectivity–behavior relationship for pre-SMA were highly similar whether based on SSRT or SSD. In addition, **Figure 4** shows that the clusters that exhibited a significant RSFC–behavior relationship for the pre-SMA seed were located in so-called "transition zones" located between overall positive and negative RSFC of the pre-SMA seed.

CONNECTIVITY–BEHAVIOR RELATIONSHIPS MODULATED BY DIAGNOSIS

We further assessed whether connectivity–behavior relationships were modulated by the presence or absence of ADHD. This was achieved by including a diagnosis-by-behavior interaction for

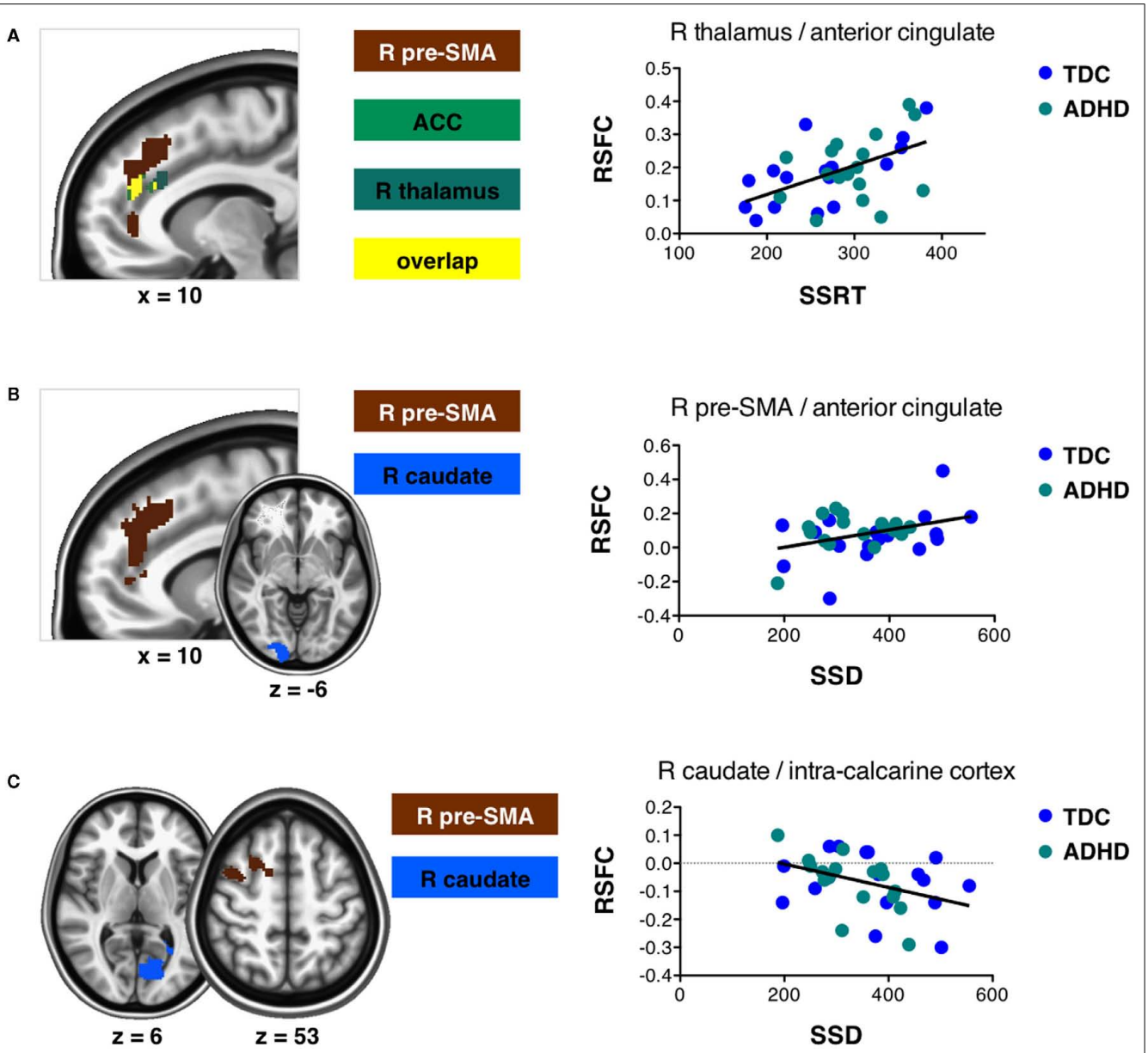

FIGURE 3 | Connectivity–behavior relationships across participants for SSRT and SSD. Slices display regions exhibiting a significantly positive or negative relationship across participants between resting state functional connectivity (RSFC) and the SSRT **(A)** or SSD **(B,C)** measures obtained from the stop signal task ($Z > 2.3$; $p < 0.05$, corrected for multiple comparisons). **(A)** Regions exhibiting a significantly positive relationship between RSFC and SSRT. **(B)** Regions exhibiting a significantly positive relationship between RSFC and SSD. **(C)** Regions exhibiting a significantly negative relationship between RSFC and SSD. Graphs illustrate example relationships. Data points are shown for typically developing children (TDC) and children with ADHD. R, right; pre-SMA, pre-supplementary motor area; ACC, anterior cingulate cortex.

each behavioral measure in the group-level analysis. For both SSRT and SSD, diagnosis-by-behavior interactions revealed several dissociations.

For SSRT, diagnosis-by-behavior interactions were found for the left insula, left thalamus, and right pre-SMA seeds (**Figure 5**). In children with ADHD, functional connectivity between right pre-SMA and right SMA, right supramarginal gyrus and parietal operculum cortex was increased in children exhibiting slower SSRTs. In contrast, TDC showed no effect. Similar interactions were obtained for functional connectivity between left insula and left putamen and right caudate. The reverse interaction, i.e., decreasing connectivity with decreased SSRT in TDC compared to decreasing connectivity with increased SSRT in ADHD, was found for functional connectivity between left thalamus and the right cerebellum.

Diagnosis-by-behavior interactions involving SSD were found for the right pre-SMA, left insula, right supramarginal gyrus, and ACC seeds (**Figures 5C,D**). Functional connectivity with right

Table 4 | MNI152 coordinates and Harvard–Oxford Atlas regions associated with all effects of interest.

Effect of interest	Seed ROI	Cluster size	*Z*-value	MNI coordinates			Region
				x	*y*	*z*	
SSRT POSITIVE							
	ACC	663	3.48	−10	42	22	Paracingulate gyrus
	R pre-SMA	983	3.93	−12	30	42	Superior frontal gyrus
	R thalamus	723	3.68	−22	8	−2	Putamen
SSD POSITIVE							
	R caudate	573	3.59	24	−92	−14	Occipital pole
	R pre-SMA	1798	4.05	−10	42	26	Paracingulate gyrus
SSD NEGATIVE							
	R caudate	794	3.75	−8	−76	6	Intracalcarine cortex
	R pre-SMA	779	4.11	34	2	40	Middle frontal gyrus
SSRT × DIAG							
	L insula	990	3.71	−28	0	−6	Putamen
	R pre-SMA						
	1	1498	3.75	46	−30	38	Supramarginal gyrus
	2	935	3.41	2	4	40	Cingulate gyrus
	L thalamus	850	3.69	20	−70	−24	Cerebellum
SSD × DIAG							
	ACC	668	3.49	22	32	36	Superior frontal gyrus
	L insula	770	3.47	−22	−8	16	Putamen
	R pre-SMA						
	1	1108	3.69	52	−34	36	Supramarginal gyrus
	2	1016	3.76	30	−64	−14	Occipital fusiform gyrus
	R supramarginal gyrus	1234	3.8	22	−66	−2	Lingual gyrus
ADHD > TDC							
	R caudate						
	1	3408	4.29	48	18	−4	Frontal operculum
	2	1304	4.05	−60	−26	8	Planum temporale
	3	1177	4.01	−32	50	36	Frontal pole
	4	916	4.36	−38	10	4	Frontal operculum
	5	805	3.95	6	26	26	Cingulate gyrus
	R frontal operculum	1274	4.32	8	10	4	Caudate
	R supramarginal gyrus						
	1	1783	4.31	10	12	6	Caudate
	2	769	3.8	12	32	24	Cingulate gyrus
	L thalamus						
	1	1853	4.87	−56	−44	10	Supramarginal gyrus
	2	973	4.57	−30	8	26	Middle frontal gyrus
	R thalamus						
	1	1009	3.75	−22	40	26	Frontal pole
	2	978	3.74	−54	−42	−4	Middle temporal gyrus
ADHD < TDC							
	L caudate	1092	3.86	2	10	−12	Subcallosal cortex
	R frontal operculum	1028	3.74	2	−48	62	Precuneus
	L thalamus	1338	3.97	2	−72	−12	Cerebellum

Coordinates are indicated for the location of the peak Z-value in each significant cluster. Correction for multiple comparisons was done using Gaussian random field theory with $Z > 2.3$ and $p < 0.05$ corrected.

pre-SMA showed the most extensive interactions including clusters in lateral occipital cortex and supramarginal gyrus. Increased negative connectivity with lateral occipital cortex was associated with longer SSD in children with ADHD, but not in TDC. Pre-SMA connectivity with supramarginal gyrus was lower in TDC exhibiting longer SSD relative to TDC exhibiting shorter SSD. The opposite was true for children with ADHD. Functional connectivity between ACC and right superior frontal gyrus decreased in

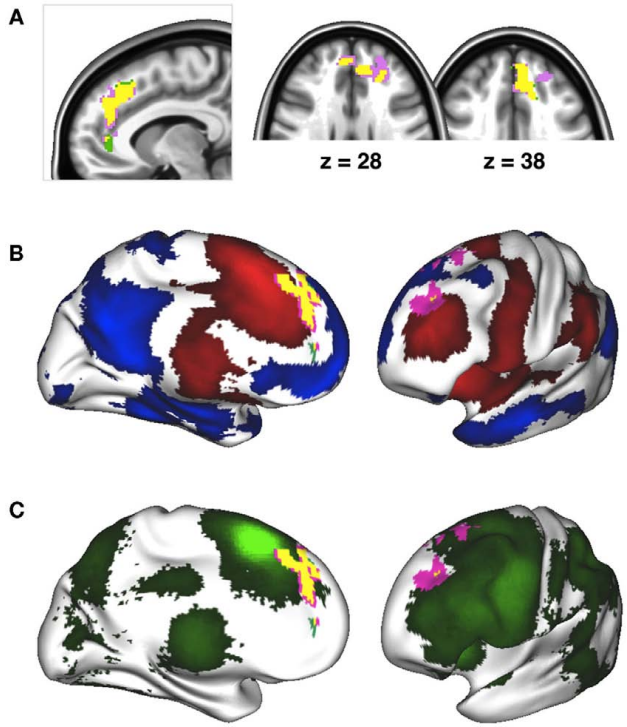

FIGURE 4 | (A) Inter-individual differences in SSRT and SSD both modulated resting state functional connectivity between right pre-supplementary motor area (pre-SMA) and a similar cluster in anterior cingulate cortex/superior frontal gyrus. Yellow indicates overlap between the cluster exhibiting a significant connectivity–behavior relationship for SSRT (grass green) and the cluster exhibiting a significant connectivity–behavior relationship for SSD (pink). **(B)** Overlap between the connectivity–behavior clusters shown in **(A)** and the overall positive (red) and negative (blue) functional connectivity network maps obtained for the pre-SMA seed. The connectivity–behavior cluster was located in transition zones between areas of overall positive or negative connectivity. **(C)** Overlap between connectivity–behavior clusters shown in **(A)** and a pre-SMA task-based co-activation map obtained from www.neurosynth.org. The co-activation map is based on a meta-analysis of activation coordinates reported together with the coordinates of the pre-SMA seed region (Yarkoni et al., 2011).

children with ADHD exhibiting longer SSD, while there was no RSFC–SSD relationship for TDC. Finally, connectivity between left insula and bilateral putamen decreased with increased SSD in TDC, while no RSFC–SSD relationship was observed for children with ADHD.

MAIN EFFECTS OF DIAGNOSIS

Figure 6 shows regions whose functional connectivity was modulated by diagnosis. We observed regions where connectivity was increased in children with ADHD relative to TDC (**Figure 6A**) as well as regions where connectivity was increased for TDC relative to children with ADHD (**Figure 6B**).

Several seeds exhibited increased connectivity strength in ADHD relative to no or weak connectivity in TDC. The right supramarginal gyrus and right caudate exhibited increased connectivity with a similar cluster in anterior cingulate cortex in children with ADHD relative to TDC. The supramarginal gyrus showed the same effect for a cluster in posterior cingulate cortex. In addition, the right frontal operculum exhibited increased connectivity with bilateral caudate in ADHD relative to TDC. A similar observation was made for the right caudate seed, whose local connectivity as well as connectivity strength with the left caudate was increased in ADHD relative to TDC. Finally, connectivity between left thalamus and left middle frontal gyrus as well as left superior temporal gyrus was increased in children with ADHD relative to no connectivity in TDC.

In contrast to these results, connectivity between the left caudate seed and ventromedial prefrontal cortex was absent in children with ADHD whereas it was significantly positive in TDC. The same effect was observed for connectivity between left thalamus and lingual gyrus. We observed no significant connectivity between frontal operculum and the right sensory–motor subdivision of the precuneus in TDC, but increased negative connectivity in ADHD.

For each cluster that showed a significant effect of diagnosis, we assessed the relationship between RSFC and ADHD-related measures obtained with the CPRS-R:L. In particular, within the children with ADHD we correlated the DSM-IV Total Score, DSM-IV Inattentive Score, DSM-IV Hyperactive–Impulsive Score, Cognitive Problems/Inattention Score, Hyperactivity Score, and the ADHD Index Score with mean RSFC obtained for each cluster. No correlation survived FDR correction for multiple comparisons ($p < 0.05$).

DISCUSSION

Recent models of ADHD highlight the contributions of aberrant functional connectivity to the pathophysiology of the disorder (Liston et al., 2011). The interpretation of such disconnection models would benefit from integration with leading neuropsychological models of ADHD, though little work has yet been done in this regard. Here, we took steps toward this goal by investigating the functional connectivity correlates of inhibitory performance during a SST and by assessing the effect of ADHD on those connections. Our findings highlight several novel brain–behavior relationships that warrant further investigation for their role in the inhibitory deficits associated with ADHD.

Previous studies have suggested that several characteristics of the brain's resting state functional architecture are relevant for understanding relationships between brain functional organization and behavior. We can apply two recently documented characteristics to the current findings. First, we recently highlighted the importance of so-called "transition zones" between an ROI's positive and negative functional connectivity networks (Mennes et al., 2010). Those transition zones are characterized by increased between-participant variability in connectivity strength and valence – regions at the boundaries of the networks might be positively connected to the ROI in some individuals, but negatively connected in others, resulting in overall non-significant connectivity. We previously found that this variability in network boundaries was predictive of the magnitude of task-induced BOLD activity (Mennes et al., 2010). In the current work regions exhibiting a significant connectivity–SSRT relationship for the pre-SMA seed

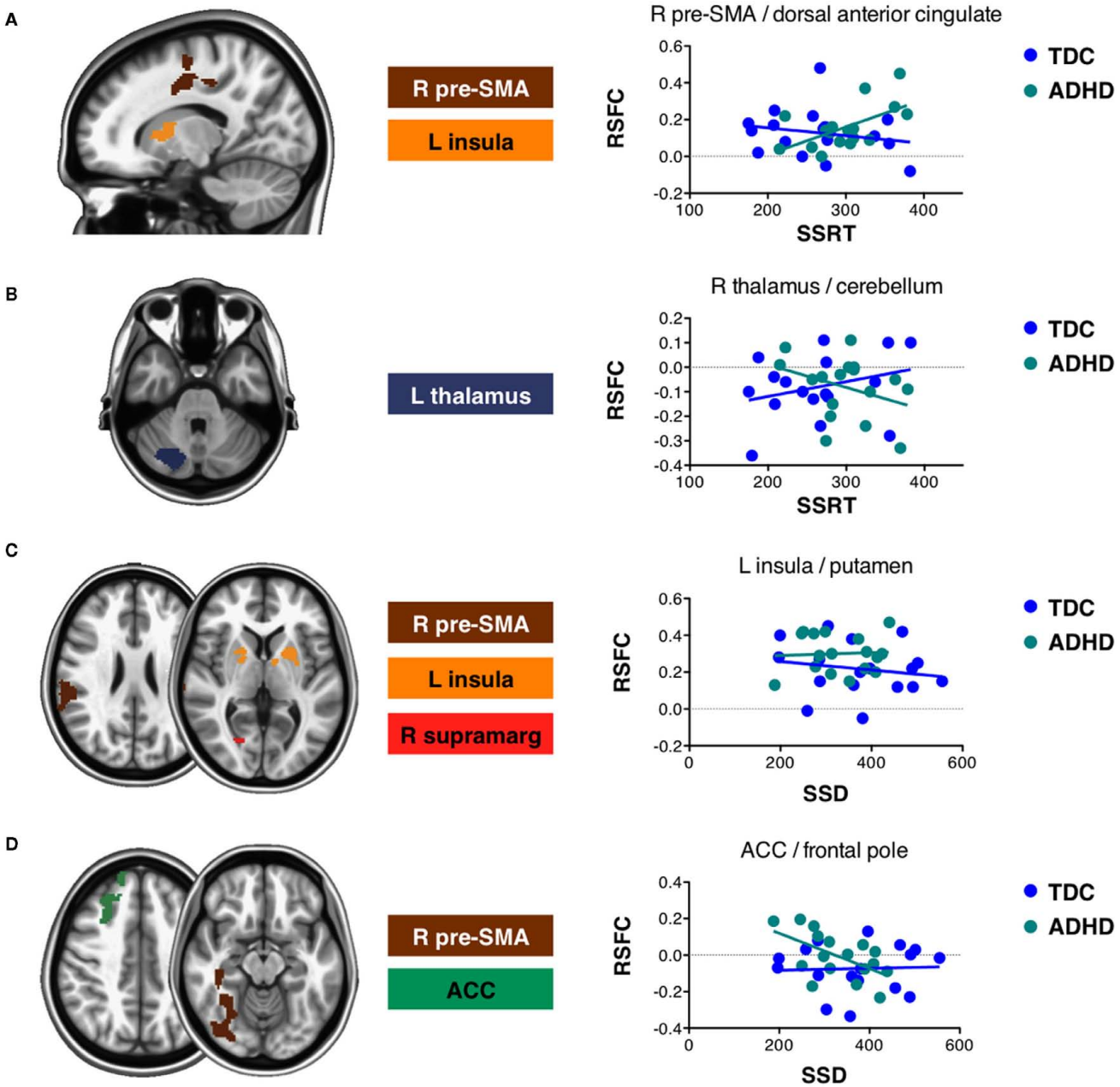

FIGURE 5 | Attention-deficit/hyperactivity disorder diagnosis modulated connectivity–behavior relationships for SSRT and SSD. Slices display regions exhibiting a significant effect of diagnosis on their connectivity–behavior relationship ($Z > 2.3$; $p < 0.05$, corrected for multiple comparisons). Interactions were observed for both SSRT and SSD obtained during the stop signal task. Graphs illustrate example interactions. **(A)** Significantly positive interactions between diagnosis and SSRT. **(B)** Significantly negative interactions between diagnosis and SSRT. **(C)** Significantly positive interactions between diagnosis and SSD. **(D)** Significantly negative interactions between diagnosis and SSD. Data points are shown for typically developing children (TDC) and children with ADHD. R, right; L, Left; pre-SMA, pre-supplementary motor area; ACC, anterior cingulate cortex; supramarg: supramarginal gyrus.

ROI were located in transition zones between regions of positive and negative connectivity (**Figure 4**). As indicated above, these transition zones exhibited slightly positive connectivity in some participants and negative connectivity in others. This observation explains why the mean of several of the observed brain–behavior relationships hovered around 0. Similar to the transition zones observed in RSFC networks, overlaying the pre-SMA clusters on a task co-activation map created by meta-analytic mining of task-based fMRI coordinates[4] (Yarkoni et al., 2011) indicated that

[4]www.neurosynth.org

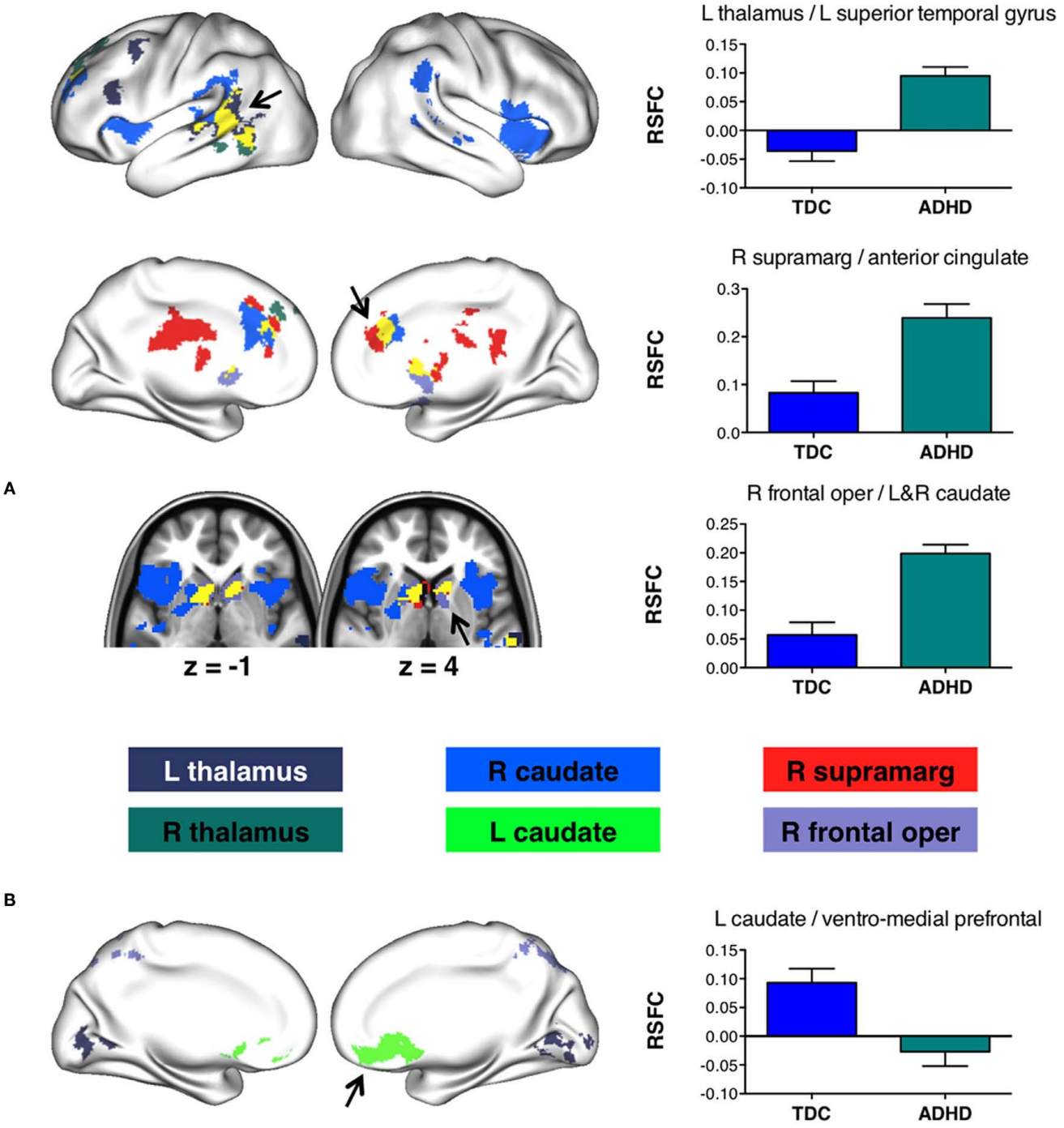

FIGURE 6 | Main effect of ADHD on resting state functional connectivity (RSFC) associated with 11 fronto-striatal seeds (Boehler et al., 2010). Surface renderings display regions exhibiting a significant main effect of diagnosis on RSFC ($Z > 2.3$; $p < 0.05$; corrected for multiple comparisons). Graphs illustrate example effects for the regions indicated by arrows on the surface renderings. **(A)** Regions exhibiting a significant ADHD > TDC effect on RSFC. **(B)** Regions exhibiting a significant ADHD < TDC effect on RSFC. R, right; L, Left; supramarg, supramarginal gyrus; frontal oper, frontal operculum.

these clusters were located on the borders of their respective task-based co-activation networks (see **Figure 4C**). Together, these findings suggest that between-subject variation in performance is linked to variation in functional network boundaries, rather than to variation in the connectivity strength of core network regions.

A second characteristic that may represent an important feature of relationships between behavior and functional brain architecture is network differentiation (Fox et al., 2005). Networks or regions are thought to be functionally differentiated if there are no correlations between them or if they are negatively correlated. This is based on the hypothesis that functional brain networks (at times) benefit from preventing cross talk between each other. For instance, participants whose brains exhibited stronger functional differentiation performed more optimally compared to participants exhibiting weaker or aberrant functional differentiation (Kelly et al., 2008; Chabernaud et al., in press). Accordingly, we observed that better differentiation between right caudate and left intracalcarine sulcus (i.e., increased negative connectivity) was associated with better inhibitory success (i.e., longer SSD; **Figure 3**). In addition, children with ADHD exhibited functional connections not observed for TDC (**Figure 6**) suggesting a less differentiated and less efficient connectivity profile (Di Martino et al., 2011).

The notion that SSRT provides the most specific index of inhibitory function has been central to most prior analyses of the SST. However, SSRT is not directly measured, but derived by subtracting SSD from the mean Go reaction time. As Alderson et al. (2007) point out, SSD should be considered when interpreting group differences in SSRT as SSD is more tightly related to inhibitory success. In the present work, we included both SSD and SSRT in the same regression model to partial out common variance associated with these two highly correlated measures. As described above, we found evidence for neural circuitry that was specifically related to either SSRT or SSD. In addition, we found neural circuitry related to SSD as well as SSRT. In particular, inter-individual differences in SSRT as well as SSD were associated with inter-individual differences in functional connectivity strength between pre-SMA and anterior cingulate cortex/superior frontal gyrus (**Figure 4**). Although SSRT and SSD are inversely related ($r = -0.81$), both RSFC/behavior relationships were positive. Therefore, rather than capturing specific aspects of the inhibition process, these results are in accordance with the observation that anterior cingulate cortex and superior frontal gyrus are activated by a variety of cognitive tasks that measure aspects of more general endogenous cognitive control (see meta-analysis Figure 1 in Mennes et al., 2006), while pre-SMA is sensitive to aspects of task difficulty and motor preparation (Milham and Banich, 2005; Stiers et al., 2010). In addition, increased pre-SMA activation has been reported in ADHD participants exhibiting higher intra-individual response speed variability, while increased superior frontal gyrus activity was observed for ADHD participants exhibiting lower intra-individual response speed variability (Suskauer et al., 2008). Further research including larger sample sizes is needed to disentangle the precise interaction between SSRT and SSD, and their relationship with RSFC. For example, short SSRT but long SSD indicate optimal inhibitory performance, yet the overlapping connectivity-behavior relationships observed for pre-SMA were positive for both SSRT and SSD.

The presence or absence of ADHD modulated connectivity–behavior relationships for both SSRT and SSD in several regions including putamen, post-central gyrus, posterior cingulate, and intracalcarine cortex. Similarly, the presence of ADHD modulated connectivity–behavior relationships for internalizing and externalizing scores obtained from the Child Behavior Checklist questionnaire (Chabernaud et al., in press). Further research is needed to unravel mechanisms underlying such differential relationships. As ADHD effects on connectivity are often interpreted in light of dysmaturational processes (Fair et al., 2010), future work should investigate age-related modulations of connectivity–behavior relationships. In the meantime, the current results suggest that ADHD should not be considered a simple extreme of brain function, since various aspects of brain function show qualitative differences depending on the presence or absence of psychopathology (Rubia et al., 2007; Chabernaud et al., in press).

Behavioral studies using the SST commonly report slower mean Go reaction times and increased reaction time variability in ADHD (see Alderson et al., 2007 and Lijffijt et al., 2005 for meta-analyses). In particular, reaction time variability has recently been put forward as an alternative phenotype for ADHD as behavioral studies have consistently demonstrated significantly higher intra-individual variability in ADHD versus neurotypical populations (Kuntsi et al., 2001; Castellanos et al., 2005; Alderson et al., 2007; Rubia et al., 2007). We did not observe a significant effect of ADHD on mean Go reaction time or reaction time variability (neither for the coefficient of variation or SD). The factors contributing to this lack of replication remain unclear and further studies are warranted. One possible reason for the absence of such effects might be the strict performance criteria used here. Yet, Nigg (1999) used the same criteria and observed an ADHD effect on reaction time variability. A second reason for the absence of such effects might be that our sample of ADHD children represents a specific neuropsychological ADHD phenotype. Accordingly, comparing our behavioral data to those reported in Nigg (1999) suggests that the ADHD children included here outperformed the ADHD children included in Nigg (1999), with faster reaction times (629 versus 713 ms) and SSRT (299 versus 405 ms). These observations are consistent with the notion that several ADHD phenotypes exist, each with their own behavioral and cognitive profile (Nigg et al., 2005).

With regard to the effects of diagnosis on functional connectivity, we replicated previous findings of ADHD-related differences in functional connectivity in ventromedial prefrontal cortex (Fair et al., 2010), and frontal operculum (Tian et al., 2006). Such findings of aberrant functional connectivity can be interpreted in terms of disrupted maturational processes (Fair et al., 2010), an interpretation that was also made in the context of functional connectivity differences in children with autism (Di Martino et al., 2011) or Tourette syndrome (Church et al., 2009). The developmental interpretation is based on observations that with maturation local connectivity (i.e., close to the seed region) decreases while long-range connectivity increases (Fair et al., 2008, 2009; Kelly et al., 2009). Similarly, we observed increased local frontal operculum connectivity and decreased long-range connectivity (e.g., left thalamus – lingual gyrus connectivity was absent in children with ADHD relative to TDC). In addition, as shown in **Figure 6**, we also observed significant effects of diagnosis in inferior frontal gyrus, anterior cingulate cortex, left dorsolateral prefrontal cortex, and insula. These

regions are known to be actively involved in higher order cognitive control operations (Koechlin et al., 2003; Brass et al., 2005; Badre and D'Esposito, 2007) and have been suggested to show differential activity in the context of ADHD (Burgess et al., 2010; Shaw et al., 2011; Spinelli et al., 2011). Interestingly, we observed these regions while assessing functional connectivity of seed ROI that were found to be related to inhibitory processing, which is in turn deemed an important aspect of cognitive control.

LIMITATIONS

Our results need to be considered in light of several limitations. Although 63 children initially participated in the study, only 34 were included in our analyses, indicating 46% data-loss. Of the omitted participants, 65% were excluded because they had a Go trial accuracy below the 75% criterion proposed by Nigg (1999). For instance, six excluded participants performed below chance level, indicating clear failure to comply with the task. One possible reason for such sub-criterion performance may be fatigue, as all children performed the SST after a 1-h long MRI scan session. In addition, the TDC were not matched to reflect the typical overrepresentation of boys among children with ADHD. However, as illustrated by **Figure 7**, our results were not driven by sex differences between both groups. Third, because of the substantial loss of analyzable data, the sample sizes were relatively small. While such sample sizes are common in neuroimaging studies of ADHD, our results warrant replication in larger sex-matched samples. Additionally, our smaller sample size might have limited our ability to detect significant behavior–connectivity relationships, especially for the clusters exhibiting a significant effect of diagnosis. Finally, we selected 11 *a priori* seed ROI for functional connectivity analyses. These were based on a prior study of the stop task and used to constrain our hypotheses, as is necessary in seed-based functional connectivity analyses (Fox and Greicius, 2010). Despite this limitation, our analyses included the whole brain, and were corrected accordingly. In the meantime, approaches for connectome wide association studies are emerging, such as graph-theory based centrality metrics (Lohmann et al., 2010; Rubinov and Sporns, 2010; Zuo et al., in press) and multivariate distance regression (Shezhad et al., oral presentation at Annual Meeting of the Organization for Human Brain Mapping, Quebec City). While the present work was motivated directly from prior findings (e.g., seed selection), future work may take advantage of these more exploratory approaches to generate novel hypotheses.

CONCLUSION

We found that two inhibitory measures derived from the SST are differentially related to functional connectivity of selected fronto-striatal seed regions. While SSRT is the traditional measure of choice, our results suggest that a different set of functional connections is related to SSD. Moreover, we showed that these functional relationships are modulated by the presence or absence of ADHD. While preliminary, our results warrant further work relating behavioral inhibition metrics to functional brain networks. Integrating neuropsychological data with emerging brain

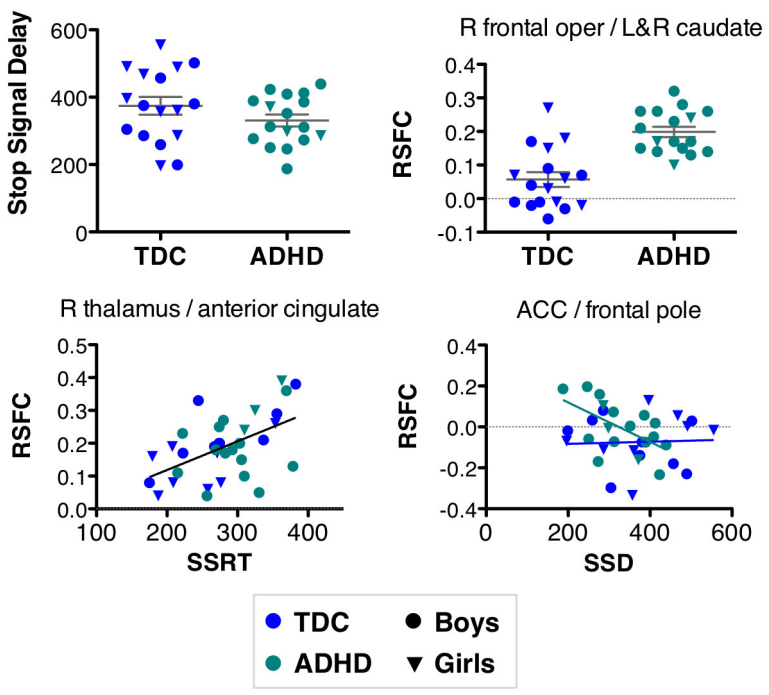

FIGURE 7 | Our results were not driven by a difference in male/female ratio between typically developing children (TDC) and children with ADHD. TDC included 8 females/9 males, while ADHD included 3 females/14 males. Graphs illustrate effects that are also shown in **Figures 2**, **6**, **3**, **5** (from left to right, top to bottom).

dysconnectivity models of ADHD will ultimately advance our understanding of the pathophysiology of this complex disorder.

ACKNOWLEDGMENTS

The authors thank all children and their parents for participating in this study. We also thank Joel Nigg for providing the stop signal task and Camille Chabernaud and Samuele Cortese for helpful comments on earlier versions of this manuscript. This research was partially supported by Grants from National Institute of Mental Health (R01MH083246 and K23MH087770), Autism Speaks, the Stavros Niarchos Foundation, the Leon Levy Foundation, and the endowment provided by Phyllis Green and Randolph Cowen. The funders had no role in study design, data collection and analysis, decision to publish, or preparation of the manuscript. Dr. Castellanos serves on the DSM-5 Workgroup on Attention-Deficit Hyperactivity and Disruptive Behavior Disorders; the views expressed in this paper are his own and do not represent those of the Workgroup or of the DSM-5 Task Force.

REFERENCES

Alderson, R. M., Rapport, M. D., and Kofler, M. J. (2007). Attention-deficit/hyperactivity disorder and behavioral inhibition: a meta-analytic review of the stop-signal paradigm. *J. Abnorm. Child. Psychol.* 35, 745–758.

Alderson, R. M., Rapport, M. D., Sarver, D. E., and Kofler, M. J. (2008). ADHD and behavioral inhibition: a re-examination of the stop-signal task. *J. Abnorm. Child. Psychol.* 36, 989–998.

Andersson, J. L. R., Jenkinson, M., and Smith, S. M. (2007). *TR07JA2: Non-linear Registration, AKA Spatial Normalisation.* FMRIB Analysis Group Technical Reports. Available at: http://www.fmrib.ox.ac.uk/analysis/techrep/

Aron, A. R., and Poldrack, R. A. (2005). The cognitive neuroscience of response inhibition: relevance for genetic research in attention-deficit/hyperactivity disorder. *Biol. Psychiatry* 57, 1285–1292.

Badre, D., and D'Esposito, M. (2007). Functional magnetic resonance imaging evidence for a hierarchical organization of the prefrontal cortex. *J. Cogn. Neurosci.* 19, 2082–2099.

Boehler, C. N., Appelbaum, L. G., Krebs, R. M., Hopf, J. M., and Woldorff, M. G. (2010). Pinning down response inhibition in the brain – conjunction analyses of the stop-signal task. *Neuroimage* 52, 1621–1632.

Brass, M., Derrfuss, J., Forstmann, B., and Von Cramon, D. Y. (2005). The role of the inferior frontal junction area in cognitive control. *Trends Cogn. Sci. (Regul. Ed.)* 9, 314–316.

Burgess, G. C., Depue, B. E., Ruzic, L., Willcutt, E. G., Du, Y. P., and Banich, M. T. (2010). Attentional control activation relates to working memory in attention-deficit/hyperactivity disorder. *Biol. Psychiatry* 67, 632–640.

Castellanos, F. X., Margulies, D. S., Kelly, C., Uddin, L. Q., Ghaffari, M., Kirsch, A., Shaw, D., Shehzad, Z., Di Martino, A., Biswal, B., Sonuga-Barke, E. J., Rotrosen, J., Adler, L. A., and Milham, M. P. (2008). Cingulate-precuneus interactions: a new locus of dysfunction in adult attention-deficit/hyperactivity disorder. *Biol. Psychiatry* 63, 332–337.

Castellanos, F. X., Sonuga-Barke, E. J., Scheres, A., Di Martino, A., Hyde, C., and Walters, J. R. (2005). Varieties of attention-deficit/hyperactivity disorder-related intra-individual variability. *Biol. Psychiatry* 57, 1416–1423.

Castellanos, F. X., Sonuga-Barke, E. J. S., Milham, M. P., and Tannock, R. (2006). Characterizing cognition in ADHD: beyond executive dysfunction. *Trends Cogn. Sci.* 10, 117–123.

Chabernaud, C., Mennes, M., Kelly, C., Nooner, K., Di Martino, A., Castellanos, F. X., and Milham, M. P. (in press). Integration of dimensional and categorical analyses of brain-behavior relationships in children with attention-deficit/hyperactivity disorder and healthy controls. *Biol. Psychiatry.* doi: 10.1016/j.biopsych.2011.08.013

Church, J. A., Fair, D. A., Dosenbach, N. U., Cohen, A. L., Miezin, F. M., Petersen, S. E., and Schlaggar, B. L. (2009). Control networks in paediatric Tourette syndrome show immature and anomalous patterns of functional connectivity. *Brain* 132, 225–238.

Conners, C. K., Sitarenios, G., Parker, J. D., and Epstein, J. N. (1998). The revised Conners' Parent Rating Scale (CPRS-R): factor structure, reliability, and criterion validity. *J. Abnorm. Child. Psychol.* 26, 257–268.

Cubillo, A., Halari, R., Ecker, C., Giampietro, V., Taylor, E., and Rubia, K. (2010). Reduced activation and inter-regional functional connectivity of fronto-striatal networks in adults with childhood attention-deficit hyperactivity disorder (ADHD) and persisting symptoms during tasks of motor inhibition and cognitive switching. *J. Psychiatr. Res.* 44, 629–639.

Di Martino, A., Kelly, C., Grzadzinski, R., Zuo, X. N., Mennes, M., Mairena, M. A., Lord, C., Castellanos, F. X., and Milham, M. P. (2011). Aberrant striatal functional connectivity in children with autism. *Biol. Psychiatry* 69, 847–856.

Dickstein, S. G., Bannon, K., Castellanos, F. X., and Milham, M. P. (2006). The neural correlates of attention deficit hyperactivity disorder: an ALE meta-analysis. *J. Child. Psychol. Psychiatry* 47, 1051–1062.

Fair, D. A., Cohen, A. L., Dosenbach, N. U., Church, J. A., Miezin, F. M., Barch, D. M., Raichle, M. E., Petersen, S. E., and Schlaggar, B. L. (2008). The maturing architecture of the brain's default network. *Proc. Natl. Acad. Sci. U.S.A.* 105, 4028–4032.

Fair, D. A., Cohen, A. L., Power, J. D., Dosenbach, N. U., Church, J. A., Miezin, F. M., Schlaggar, B. L., and Petersen, S. E. (2009). Functional brain networks develop from a "local to distributed" organization. *PLoS Comput. Biol.* 5, e1000381. doi:10.1371/journal.pcbi.1000381

Fair, D. A., Posner, J., Nagel, B. J., Bathula, D., Dias, T. G., Mills, K. L., Blythe, M. S., Giwa, A., Schmitt, C. F., and Nigg, J. T. (2010). Atypical default network connectivity in youth with attention-deficit/hyperactivity disorder. *Biol. Psychiatry* 68, 1084–1091.

Fox, M. D., and Greicius, M. (2010). Clinical applications of resting state functional connectivity. *Front. Syst. Neurosci.* 4:19. doi:10.3389/fnsys.2010.00019

Fox, M. D., Snyder, A. Z., Vincent, J. L., Corbetta, M., Van Essen, D. C., and Raichle, M. E. (2005). The human brain is intrinsically organized into dynamic, anticorrelated functional networks. *Proc. Natl. Acad. Sci. U.S.A.* 102, 9673–9678.

Jenkinson, M., Bannister, P. R., Brady, J. M., and Smith, S. M. (2002). Improved optimisation for the robust and accurate linear registration and motion correction of brain images. *Neuroimage* 17, 825–841.

Jenkinson, M., and Smith, S. M. (2001). A global optimisation method for robust affine registration of brain images. *Med. Image Anal.* 5, 143–156.

Kaufman, J., Birmaher, B., Brent, D., Rao, U., Flynn, C., Moreci, P., Williamson, D., and Ryan, N. (1997). Schedule for affective disorders and schizophrenia for school-age children present and lifetime version (K-SADS-PL): initial reliability and validity data. *J. Am. Acad. Child Adolesc. Psychiatry* 36, 980–988.

Kelly, A. M., Di Martino, A., Uddin, L. Q., Shehzad, Z., Gee, D. G., Reiss, P. T., Margulies, D. S., Castellanos, F. X., and Milham, M. P. (2009). Development of anterior cingulate functional connectivity from late childhood to early adulthood. *Cereb. Cortex* 19, 640–657.

Kelly, A. M., Uddin, L. Q., Biswal, B. B., Castellanos, F. X., and Milham, M. P. (2008). Competition between functional brain networks mediates behavioral variability. *Neuroimage* 39, 527–537.

Koechlin, E., Ody, C., and Kouneiher, F. (2003). The architecture of cognitive control in the human prefrontal cortex. *Science* 302, 1181–1185.

Konrad, K., Gauggel, S., Manz, A., and Scholl, M. (2000). Inhibitory control in children with traumatic brain injury (TBI) and children with attention deficit/hyperactivity disorder (ADHD). *Brain Inj.* 14, 859–875.

Kuntsi, J., Oosterlaan, J., and Stevenson, J. (2001). Psychological mechanisms in hyperactivity: I. Response inhibition deficit, working memory impairment, delay aversion, or something else? *J. Child. Psychol. Psychiatry* 42, 199–210.

Lijffijt, M., Kenemans, J. L., Verbaten, M. N., and Van Engeland, H. (2005). A meta-analytic review of stopping performance in attention-deficit/hyperactivity disorder: deficient inhibitory motor control? *J. Abnorm. Psychol.* 114, 216–222.

Liston, C., Cohen, M. M., Teslovich, T., Levenson, D., and Casey, B. J. (2011). Atypical prefrontal connectivity in attention-deficit/hyperactivity disorder: pathway to disease or pathological end point? *Biol. Psychiatry* 69, 1168–1177.

Logan, G. D., Cowan, W. B., and Davis, K. A. (1984). On the ability to inhibit simple and choice reaction time responses: a model and a method. *J. Exp. Psychol. Hum. Percept. Perform.* 10, 276–291.

Logan, G. D., Schachar, R. J., and Tannock, R. (1997). Impulsivity and inhibitory control. *Psychol. Sci.* 8, 60–64.

Lohmann, G., Margulies, D. S., Horstmann, A., Pleger, B., Lepsien, J., Goldhahn, D., Schloegl, H., Stumvoll, M., Villringer, A., and Turner, R. (2010). Eigenvector centrality mapping for analyzing connectivity patterns in fMRI data of the human brain. *PLoS ONE* 5, e10232. doi:10.1371/journal.pone.0010232

Mennes, M., Kelly, C., Zuo, X. N., Di Martino, A., Biswal, B., Xavier Castellanos, F., and Milham, M. P. (2010). Inter-individual differences in resting state functional connectivity predict task-induced BOLD activity. *Neuroimage* 50, 1690–1701.

Mennes, M., Stiers, P., Lagae, L., and Van Den Bergh, B. (2006). Long-term cognitive sequelae of antenatal maternal anxiety: involvement of the orbitofrontal cortex. *Neurosci. Biobehav. Rev.* 30, 1078–1086.

Milham, M. P., and Banich, M. T. (2005). Anterior cingulate cortex: an fMRI analysis of conflict specificity and functional differentiation. *Hum. Brain Mapp.* 25, 328–335.

Nigg, J. T. (1999). The ADHD response-inhibition deficit as measured by the stop task: replication with DSM-IV combined type, extension, and qualification. *J. Abnorm. Child. Psychol.* 27, 393–402.

Nigg, J. T. (2001). Is ADHD a disinhibitory disorder? *Psychol. Bull.* 127, 571–598.

Nigg, J. T., Willcutt, E. G., Doyle, A. E., and Sonuga-Barke, E. J. (2005). Causal heterogeneity in attention-deficit/hyperactivity disorder: do we need neuropsychologically impaired subtypes? *Biol. Psychiatry* 57, 1224–1230.

Power, J. D., Barnes, K. A., Snyder, A. Z., Schlaggar, B. L., and Petersen, S. E. (in press). Spurious but systematic correlations in functional connectivity MRI networks arise from subject motion. *Neuroimage*. http://dx.doi.org/10.1016/j.neuroimage.2011.10.018

Rubia, K., Overmeyer, S., Taylor, E., Brammer, M., Williams, S. C., Simmons, A., and Bullmore, E. T. (1999). Hypofrontality in attention deficit hyperactivity disorder during higher-order motor control: a study with functional MRI. *Am. J. Psychiatry* 156, 891–896.

Rubia, K., Smith, A. B., Brammer, M. J., and Taylor, E. (2007). Temporal lobe dysfunction in medication-naive boys with attention-deficit/hyperactivity disorder during attention allocation and its relation to response variability. *Biol. Psychiatry* 62, 999–1006.

Rubinov, M., and Sporns, O. (2010). Complex network measures of brain connectivity: uses and interpretations. *Neuroimage* 52, 1059–1069.

Shaw, P., Gilliam, M., Liverpool, M., Weddle, C., Malek, M., Sharp, W., Greenstein, D., Evans, A., Rapoport, J., and Giedd, J. (2011). Cortical development in typically developing children with symptoms of hyperactivity and impulsivity: support for a dimensional view of attention deficit hyperactivity disorder. *Am. J. Psychiatry* 168, 143–151.

Spinelli, S., Joel, S., Nelson, T. E., Vasa, R. A., Pekar, J. J., and Mostofsky, S. H. (2011). Different neural patterns are associated with trials preceding inhibitory errors in children with and without attention-deficit/hyperactivity disorder. *J. Am. Acad. Child Adolesc. Psychiatry* 50, 705.e3–715.e3.

Stiers, P., Mennes, M., and Sunaert, S. (2010). Distributed task coding throughout the multiple demand network of the human frontal-insular cortex. *Neuroimage* 52, 252–262.

Suskauer, S. J., Simmonds, D. J., Fotedar, S., Blankner, J. G., Pekar, J. J., Denckla, M. B., and Mostofsky, S. H. (2008). Functional magnetic resonance imaging evidence for abnormalities in response selection in attention deficit hyperactivity disorder: differences in activation associated with response inhibition but not habitual motor response. *J. Cogn. Neurosci.* 20, 478–493.

Tian, L., Jiang, T., Wang, Y., Zang, Y., He, Y., Liang, M., Sui, M., Cao, Q., Hu, S., Peng, M., and Zhuo, Y. (2006). Altered resting-state functional connectivity patterns of anterior cingulate cortex in adolescents with attention deficit hyperactivity disorder. *Neurosci. Lett.* 400, 39–43.

Van Dijk, K. R., Sabuncu, M. R., and Buckner, R. L. (2012). The influence of head motion on intrinsic functional connectivity MRI. *Neuroimage* 59, 431–438.

Yarkoni, T., Poldrack, R. A., Nichols, T. E., Van Essen, D. C., and Wager, T. D. (2011). Large-scale automated synthesis of human functional neuroimaging data. *Nat. Methods* 8, 665–670.

Zuo, X., Ehmke, R., Mennes, M., Imperati, D., Castellanos, F. X., Sporns, O., and Milham, M. P. (in press). Network centrality and information flow in the human brain functional connectome. *Cereb. Cortex*. doi: 10.1093/cercor/bhr269

Conflict of Interest Statement: The authors declare that the research was conducted in the absence of any commercial or financial relationships that could be construed as a potential conflict of interest.

Received: 30 September 2011; accepted: 28 December 2011; published online: 11 January 2012.

Citation: Mennes M, Vega Potler N, Kelly C, Di Martino A, Castellanos FX and Milham MP (2012) Resting state functional connectivity correlates of inhibitory control in children with attention-deficit/hyperactivity disorder. Front. Psychiatry ***2****:83. doi: 10.3389/fpsyt.2011.00083*

This article was submitted to Frontiers in Neuropsychiatric Imaging and Stimulation, a specialty of Frontiers in Psychiatry.

APPENDIX

As described in Van Dijk et al. (2012) and Power et al. (in press), micromovements that occur during a resting state fMRI scan, can significantly influence measures and results derived from this scan. One suggestion to deal with such movements involves removing timepoints that exceed a threshold for excessive movement from the resting state time series before calculating any derived measures, this procedure is referred to as "scrubbing" (Power et al., in press). While easily adoptable for task-based fMRI scans, more research is needed to assess the effect of removing timepoints from analyses that investigate frequency measures or that focus on a certain frequency in the BOLD signal, as is the case for resting state functional connectivity.

The participants included in our manuscript exhibited limited movement during their resting state scan. Yet, here we present our main results while comparing analyses based on the original data versus analyses based on data after scrubbing timepoints contaminated with micromovements exceeding 0.5 mm framewise displacement (see Power et al., in press, for details).

Scrubbing our data according to the Power et al. (in press) method had very little impact on our results. Nineteen out of the 34 subjects needed scrubbing; of those only 4 needed more than 5% of frames (i.e., more than 10 frames) scrubbed (see **Figure A1**). The maximum number of frames scrubbed was: 18% (i.e., 33 frames). For each of the 11 seed ROI and effects of interest we observed very high correlations between the *Z*-statistic maps obtained with and without scrubbing. In fact, for each of the 55 *Z*-statistic maps we assessed (11 seed ROI, 5 contrasts), correlations exceeded 0.98. In addition, the maximum mean absolute difference in pre- and post-scrubbing *Z*-statistic values was 0.14, with a max SD of 0.12. The maximum absolute pre-/post-scrubbing difference in these 55 *Z*-statistic maps was 1.67. Together, these results suggests that, at the group level, scrubbing for micromovements had little impact on our statistical maps and did not alter the topography of our results (see **Figure A2**).

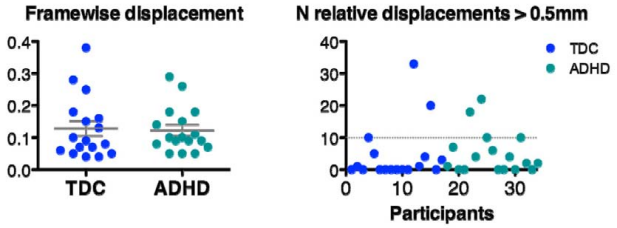

FIGURE A1 | Framewise displacement and *N* relative displacements calculated according to Power et al. (in press).

These results indicate limited variation in the pre/post-scrubbing *Z*-statistic maps. Although limited, such variations might cause some voxels to pass our statistical threshold after scrubbing while others, that passed pre-scrubbing, are now below that threshold. However, given the 0.98 correlation between pre/post-scrubbing *Z*-statistic values, it is clear that the topography of effects was not fundamentally altered after scrubbing. Across our effects of interest we observed 31 clusters in the data before scrubbing, and 33 in the scrubbed data. While six clusters disappeared by scrubbing, seven new clusters appeared. In the figures below we illustrate the observed effect for four ROI, two were significant before scrubbing, but not after scrubbing, while two were significant after scrubbing, but not present in the original, unscrubbed analyses. Yet, from **Figure A3** it is clear that for all clusters the effects of interest were highly similar pre/post-scrubbing, indicating that differences in cluster significance between the unscrubbed and scrubbed analyses were merely due to minor threshold changes at single voxels.

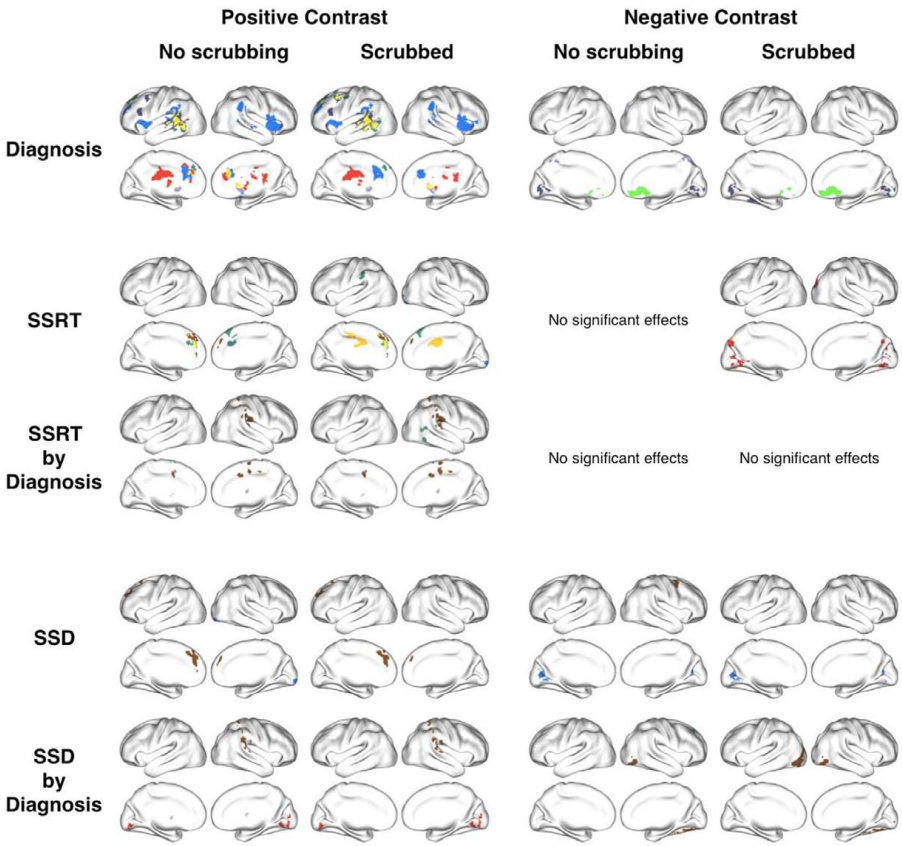

FIGURE A2 | Scrubbing timepoints containing micromovements from each participants' resting state timeseries had limited impact on our results. This figure shows the surface plots for each effect of interest for analyses using data without scrubbing (as reported in our manuscript) and analyses using scrubbed data.

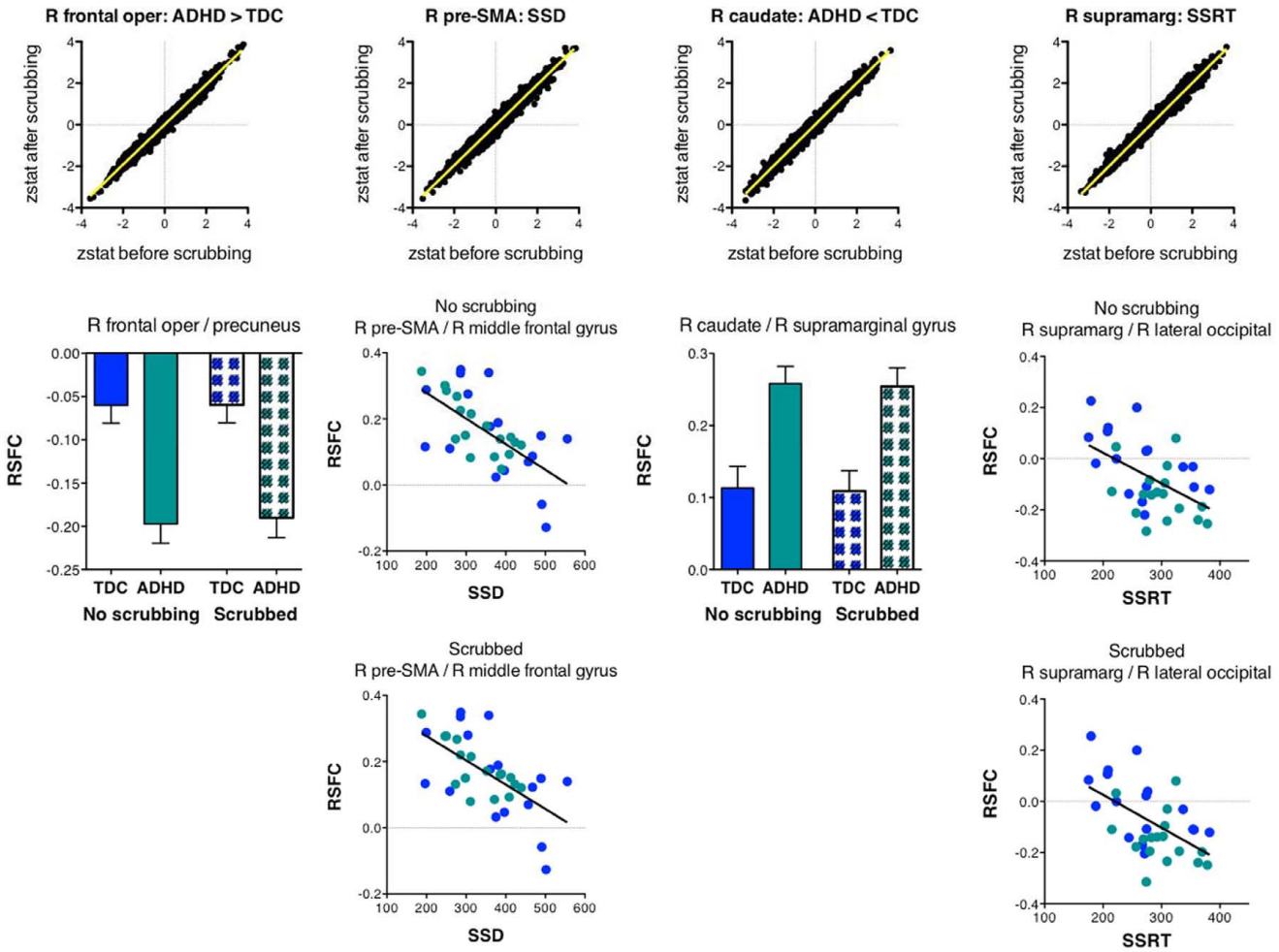

FIGURE A3 | Scrubbing the data for micromovements had limited impact on the *Z*-statistic values (*z*stat) and effects of interest obtained prior to scrubbing. This figure shows data for four clusters. The two clusters shown on the left reached significance in the analyses that used unscrubbed data, but were not significant at the whole-brain FWE corrected level in the analyses using the scrubbed data. In contrast, the two clusters on the right "appeared" in the analyses using the scrubbed data, but did not reach cluster significance in the analyses using unscrubbed data. For each cluster (column) the top row illustrates the similarity between the *Z*-statistic values of the effect of interest obtained for the analyses using unscrubbed and scrubbed data.